# *4 Zirconia substituted 1393 bioactive glass Hydroxyapatite composite system*

## 4.1 Introduction

Composites are defined as the heterogeneous combination of two or more materials having different compositions, morphology and physical properties at a macroscopic level. The aim is to develop these materials having properties that cannot be obtained from a single material. However, its application in the biomedical industry is still very less than expected. Hydroxyapatite from calcium phosphate group has a similar mineral composition to the bone and has a Ca/P ratio equal to 1.67 with a density of 3.16 $g/cm^3$ (Goller et al., 2003). Due to its biocompatibility and excellent osteoconductivity, it has wide applications in dental and orthopedic surgery. The main disadvantage is its poor mechanical strength which limits its use for load-bearing applications in bulk form. Due to this restriction, it is generally used in cement, and as a coating material over metallic implants (Bellucci et al., 2017). Hydroxyapatite is bioactive material but its reactivity and integration with bone tissue are very low. Low degradability of hydroxyapatite implant in the physiological environment restricts its replacement or resorption by new bone which leads to failure at an interface or in an implant. This failure can be overcome by reinforcing hydroxyapatite with a bioactive glass (Bellucci et al., 2015). Bioactive glasses have a higher bioactivity than hydroxyapatite and form good bonding with neighboring bone. Their bioactivity can be explained both in-vivo and in-vitro conditions (Goller et al., 2003). Released ions from bioactive glasses promote cell growth, improve osteoblast and angiogenesis process. Bone forming ability of bioactive glass is very fast, and it forms a new bond in few hours but brittleness of bioactive glasses limits its application in tissue engineering scaffold (So et al., 2006). Goller et al., 2003 demonstrated the behavior of 45S5 glass/hydroxyapatite composite with different sintering temperatures and found that high-temperature sintering promoted undesirable phase of $Na_2HPO_4 \cdot 7H_2O$ and decomposition of hydroxyapatite with bioactive glass decreased the mechanical properties. However, osteoconductive behavior of hydroxyapatite promoted

osteogenic of marrow stromal cells. While in terms of bioactivity and osteoblastic, it took longer duration than large marrow stromal cells. To promote bioactivity of hydroxyapatite, different ceramics and bioglass were added as sintering aid (Demirkiran et al., 2010). Chatzistavrou et al., 2006 suggested that sintering promotes the bioactivity of sintered 45S5/hydroxyapatite composites. Besides bioglass, sodium phosphate in the hydroxyapatite bioglass system promotes bioactivity. The reaction of bioglass with hydroxyapatite at higher sintering temperature also deteriorates density which affects mechanical strength. To enhance bioactivity, variation in bioglass chemistry or sintering method should be adopted (Bellucci et al., 2015).

Yadav et al., 2017 have studied the effect of zirconia substitution in 1393 bioactive glass on bioactivity and mechanical properties. In this study, zirconia substituted 1393 bioactive glass with hydroxyapatite biocomposite system was sintered at 600°C and 1000°C respectively. At 600°C only hydroxyapatite phase was formed whereas at 1000°C Akermanite with Hydroxyapatite was formed. The present investigation was carried out to study the effect of hydroxyapatite on bioactivity, mechanical properties, and cell proliferation. The phases were characterized by XRD and FTIR. Effect of sintering temperature on properties of density, compressive strength, in-vitro bioactivity, and cell proliferation was studied. To measure biocompatibility, MG63 cell lines were cultured on sintered composites in 96 well plate and cell proliferation after 2 and 7days was investigated using MTT assay.

## 4.2 Materials and method

### 4.2.1 Synthesis of bioglass

Zirconia substituted 1393 bioactive glass was synthesized by the sol-gel method. The required amount of TEOS was added into 20 ml of 0.1 N $HNO_3$ solutions and stirred for

45 min to complete the hydrolysis reaction. TEP, ($Ca(NO_3)_2 \cdot 4H_2O$), Magnesium nitrate hexahydrate, Sodium nitrate, Potassium nitrate, and Zirconium oxynitrate hydrate were added in the required amount and stirred for 45 min individually to obtain a transparent sol. Sol was aged at room temperature for hydrolysis and polycondensation reaction until gel formation takes place. The gel was dried at 60°C for 24hr. The dried gel was thermally treated at 600°C to obtain the amorphous nature of glass.

### 4.2.2 Hydroxyapatite synthesis

Highly crystalline hydroxyapatite powder was prepared by the co-precipitation method The solution of Calcium hydroxide was stirred for 15 min. Further, the solution of Di-ammonium hydrogen orthophosphate was added and stirred for another 15 min. pH of the solution was kept at 9 by adding 0.1 N NaOH solution. The solution was further stirred for another 60 min. The solution was filtered and washed several times. The precipitate was dried in an oven at 60°C for 24hr. The dried powder was sintered at 1000°C for 6 h.

### 4.2.3 Biocomposite preparation

To prepare biocomposite, hydroxyapatite powder in the different ratios was mixed with a substituted bioactive glass (amount listed in **Table 4.1**) and heat-treated at two temperatures 600°C and 1000°C for 6 h to evaluate the changes in phase and structure. Bioglass with the different weight ratio of hydroxyapatite powder was wet-milled. The powder was dried and sintered at 600°C and 1000°C for 6 h.

**Table 4.1** Composition of bioglass/hydroxyapatite composite.

| Sample Code | Hydroxyapatite (wt. %) | Bioactive glass (wt. %) |
|---|---|---|
| BG_H0 | 0 | 100 |
| BG_H20 | 20 | 80 |

| | | |
|---|---|---|
| BG_H50 | 50 | 50 |
| BG_H80 | 80 | 20 |

## 4.3 Characterization and test

Simultaneous Thermal analysis (STA) was performed to analyze the crystallization and stability behavior of biocomposite. For this, samples were heated from 27-1000°C at the rate of 10°C/min in a nitrogen atmosphere. To analyze the phases present in bioglass, hydroxyapatite and composite system, X-ray diffraction was performed with 2θ range from 20 to 80° (step size = 0.02° and step time = 2s) using CuKα radiation. For microstructure analysis, scanning electron microscopy was performed on samples after SBF immersion. To analyze the functional groups present in the composite samples, ATR FTIR was used and the spectrum was recorded in a range of 400-4000 $cm^{-1}$ wave number.

For in-vitro bioactivity analysis, powders were soaked in SBF solution for 3, 5, 7, 14, 21 and 28 days in an incubator at 37°C. The ratio of SBF solution to powder was kept 100:1 (Pramanik et al., 2015). SBF solution was prepared according to Kokubo et al., 2006 with an initial pH value of 7.4. SBF has composition and concentration similar to blood plasma. After a defined soaking period, powders were removed from the solution and the pH of the solution was measured. After this, wet powders were dried and apatite layer formation over the sample surface was characterized by XRD, FTIR, and SEM techniques.

The bulk density of sintered composite samples was determined by Archimedes' principle in the water medium. Triplicate of each sample was used to measure the average density. The compression strength of composite samples was performed on Tinius Olsen H10KL with a crosshead speed of 0.5 mm/min. Triplicate of each composition was prepared to measure the average compressive strength (Ragel et al., 2002).

Biocompatibility analysis of sintered composites was analyzed over MG-63 cell lines obtained from NCCS Pune, India. In this test, the yellow color tetrazolium reduced into purple formazan. The spectrophotometric method was used to quantify this intracellular purple color formazan. The cell growth was reciprocal to the reduction rate of yellow color tetrazolium. This test was performed according to procedure described in **section 3.8.1**.

## 4.4 Statistical Analysis:

For in-vitro cell proliferation, triplicates of each sample were performed and data were presented as mean with standard deviation (mean ± SD). The one-way ANOVA test followed by Tukey's post hoc test was used for significance differences (p-value < 0.05). The symbol '*', 'θ', '#', 'σ' represent statistically significant difference at p-value < 0.05 from control, composite BG_20, BG_50, and BG_80 (sintered at 600°C) respectively. For composites BG_20, BG_50, BG_80 (sintered at 1000°C), symbol 'α', '*v*' and 'δ' were selected respectively.

## 4.5 Results and discussion

### 4.5.1 Simultaneous Thermal analysis (STA)

To study the thermal stability and thermal behaviour of composites STA was performed. **Figure 4.1(a)** and **Figure 4.1(b)** show the DSC and TGA graph of bioglass/hydroxyapatite composite before the sintering process. In the DSC curve (**Figure 4.1(a)**), an exothermic peak was started from 960°C that shows the crystallization ($T_c$) would start in composite samples. A small peak around at a temperature of 600°C was found which attributed to glass transition temperature ($T_g$) in composite samples.

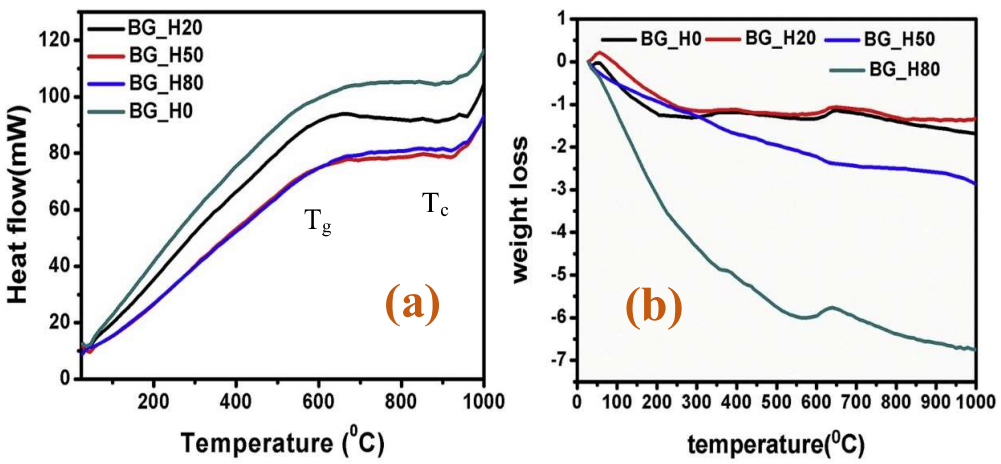


**Figure 4.1 (a)** DSC and **(b)** TGA graphs of bioglass/hydroxyapatite composite before the sintering process

In the TGA graph (**Figure 4.1(b)**), different stages of weight loss were found in composite samples. Liao et al., 1999 stated that the hydroxyapatite powder quickly loses weight when the temperature ranges between 100-400°C**.** There is no apparent weight change in the temperature range of 400-800°C. The weight of the hydroxyapatite powders then reduces gradually as the temperature rises to 800°C. In composite samples, weight loss in BG_H0, BG_H20, BG_H50, and BG_H80 was approximately 1.33, 1.2, 2.23 and 6% respectively. BG_H0 sample is corresponding to pure zirconia substituted bioglass. In composite samples, continuous weight loss was found. The weight loss was highest for BG_H80 compared to the other three composites.

### 4.5.2 Phase analysis

**Figure 4.2** shows the XRD pattern of zirconia substituted bioglass (BG_H0) and hydroxyapatite (HA). In the XRD pattern of BG_H0, no sharp diffraction peak is observed which suggests the amorphous structure of substituted bioglass. A broad hump at 2theta from 25° to 37° degrees shows a characteristic peak of silicate glass (Yadav et al., 2017). While

XRD pattern of hydroxyapatite produced at 1000°C shows pure hydroxyapatite phase (JCPDS No 98-004-7092) of hexagonal structure. No other phase like TCP was found.

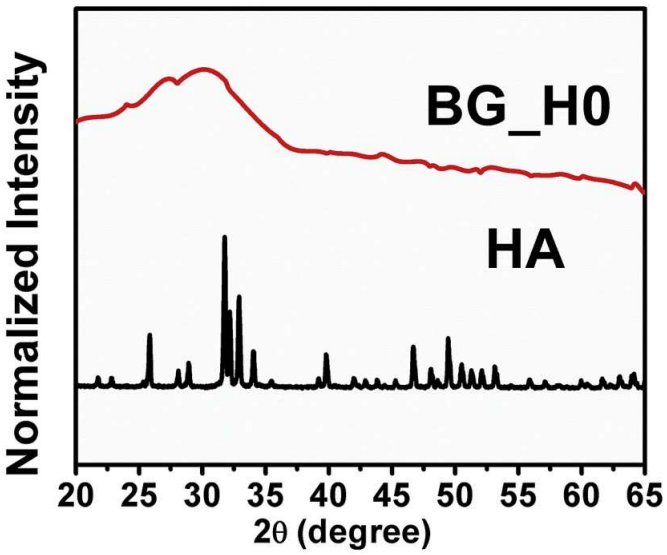


**Figure 4.2** XRD of zirconia substituted bioglass (BG_H0) and hydroxyapatite (HA).

**Figure 4.3(a)**, **Figure 4.3(b)** shows the XRD pattern of composite system heat-treated at 600°C and 1000°C for 6hrs respectively. In **Figure 4.3(a)** hydroxyapatite with hexagonal structure was found which shows that no chemical reaction between bioglass and hydroxyapatite was taking place. It was also found that the intensity of the hydroxyapatite phase increased with increasing hydroxyapatite amount in the composite samples. While in **Figure 4.3(b)** XRD pattern shows the mixed phases of hydroxyapatite with Akermanite showing the chemical reaction at this temperature (1000°C) between bioglass and hydroxyapatite. **Table 4.2** shows the phase presented after the sintering of composites.

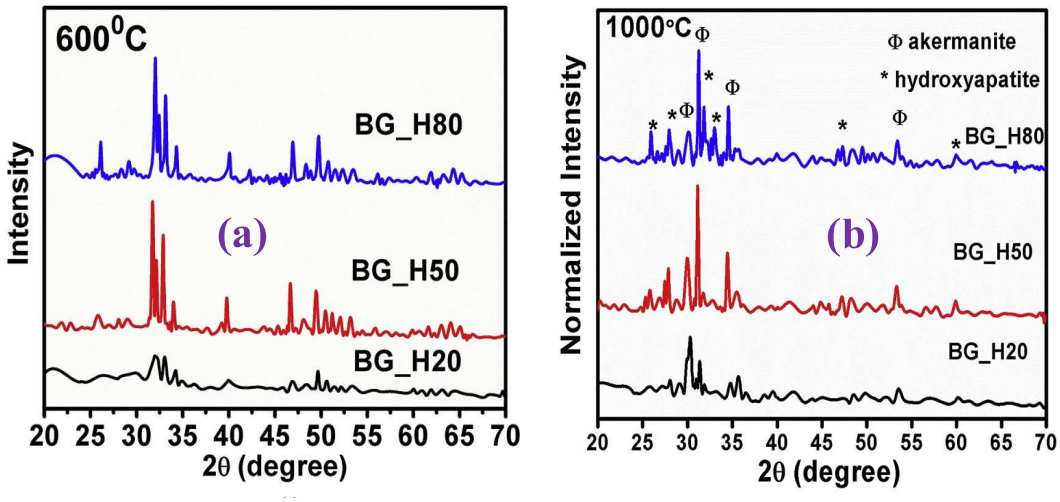


**Figure 4.3 (a)** XRD of composites heated at 600 °C and **(b)** at 1000 °C.

**Table 4.2** Phase developed after the sintering process

| Sample code | Temperature (°C) | Phase |
|---|---|---|
| **BG_H20** | 600 | Hydroxyapatite |
| **BG_H50** | 600 | Hydroxyapatite |
| **BG_H80** | 600 | Hydroxyapatite |
| **BG_H20** | 1000 | Akermanite + Hydroxyapatite |
| **BG_H50** | 1000 | Akermanite + Hydroxyapatite |
| **BG_H80** | 1000 | Akermanite + Hydroxyapatite |

### 4.5.3 Transmittance FTIR analysis

**Figure 4.4 (a)**, **Figure 4.4 (b)** shows the transmittance FTIR spectra of zirconia substituted bioglass (BG_H0) and hydroxyapatite powder (HA). BG_H0 show the characteristic peaks of silica only **(Figure 4.4 (a)).** The transmittance band at wave number of 972, 924, 863,719,634 $cm^{-1}$ corresponds to $SiO_4$ (Sadeghzade et al., 2017). Transmittance bands at 1446 $cm^{-1}$ correspond to the $CO_3^{-2}$ group formed due to the reaction of bioglass with $CO_2$ present in the atmosphere during the formation process (Solgi et al., 2017) (Pazarçeviren et al., 2018). A band at 435 $cm^{-1}$ corresponds to Si-O-Si bending (Tripathi et al., 2015).

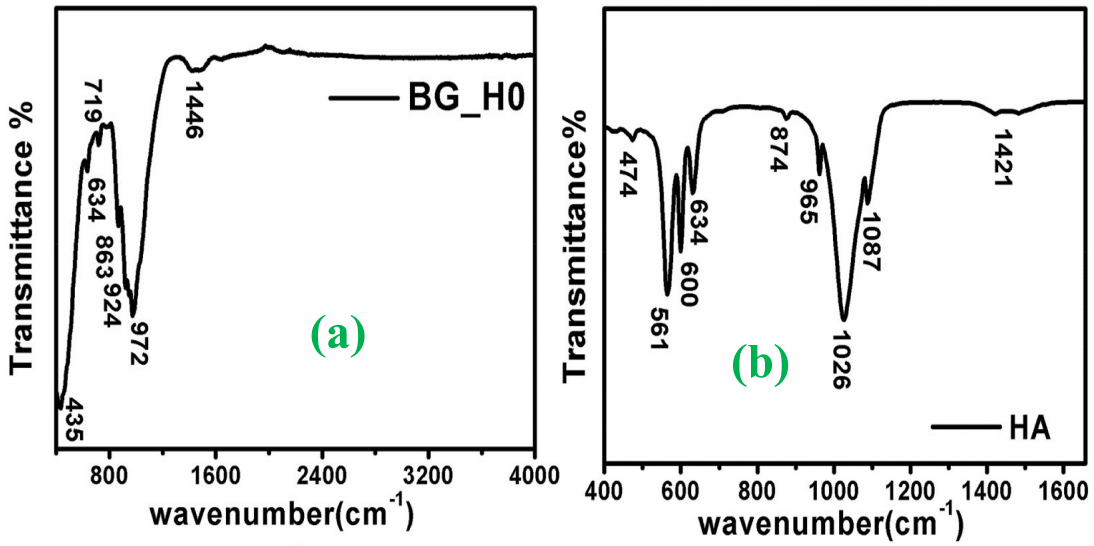


**Figure 4.4 (a)** Transmittance FTIR spectra of zirconia substituted bioglass (BG_H0) and **(b)** of hydroxyapatite (HA).

In transmittance spectra of hydroxyapatite **(Figure 4.4 (b))**, bands appearing at 474, 561 and 600 $cm^{-1}$ are related to bending mode of P-O bond (Nasker et al., 2018). The peak at 634 $cm^{-1}$ is related to stretching and vibrational modes of O-H groups (Ciobanu et al., 2013).

Peaks at 874 and 1421 $cm^{-1}$ are related to $v_2$ vibrational and stretching vibrations of the $CO_3^{-2}$ group respectively. The carbonate group is formed due to $CO_2$ present in the atmosphere (Nasker et al., 2018) (Sabu et al., 2019). The peak at 965 $cm^{-1}$ is related to symmetric stretching ($v_1$) of the P-O bond. A strong peak at 1026 $cm^{-1}$ is related to asymmetric stretching vibration mode of $PO_4^{-3}$ group which confirms the hydroxyapatite formation. Several authors reported that hydroxyapatite with carbonate has a similar composition of apatite present in bone and also with high bioactivity. The peak at 1087 and 3570 $cm^{-1}$ are related to $v_3$ ($PO_4^{-3}$) bending and stretching of the O-H group respectively present in hydroxyapatite (Sabu et al., 2019).

**Figure 4.5(a)**, **Figure 4.5(b)** depicts the transmittance FTIR spectra of bioglass/hydroxyapatite composite heat-treated at 600°C and 1000°C respectively. In **Figure 4.5(a)**, all transmittance bands are corresponding to hydroxyapatite which was also reported in the XRD pattern. In transmittance IR spectra, it was found that the intensity of bands decreased with increasing hydroxyapatite amount which might be due to the $SiO_2$ presence (Andersson et al., 2005). Also, the transmittance band corresponding to 1026 and 1090 $cm^{-1}$ shows the presence of both P-O and Si-O-Si bond. Both groups have the same vibration number; therefore, it was difficult to differentiate them due to their overlapping. The carbonate group present in the hydroxyapatite structure was also not found after the heating of composite samples. It might be due to the decomposition of hydroxyapatite with glass. At low-temperature heating, the carbonate group entered in structure with hydroxyapatite but at the higher heating temperature, it was removed due to glass reactivity with hydroxyapatite. In another way, the transmittance IR data confirms the loss of both carbonate and hydroxyl group because of the reactivity of glass with hydroxyapatite at a higher heating temperature (Chatzistavrou et al., 2006, Lopes et al., 1998).

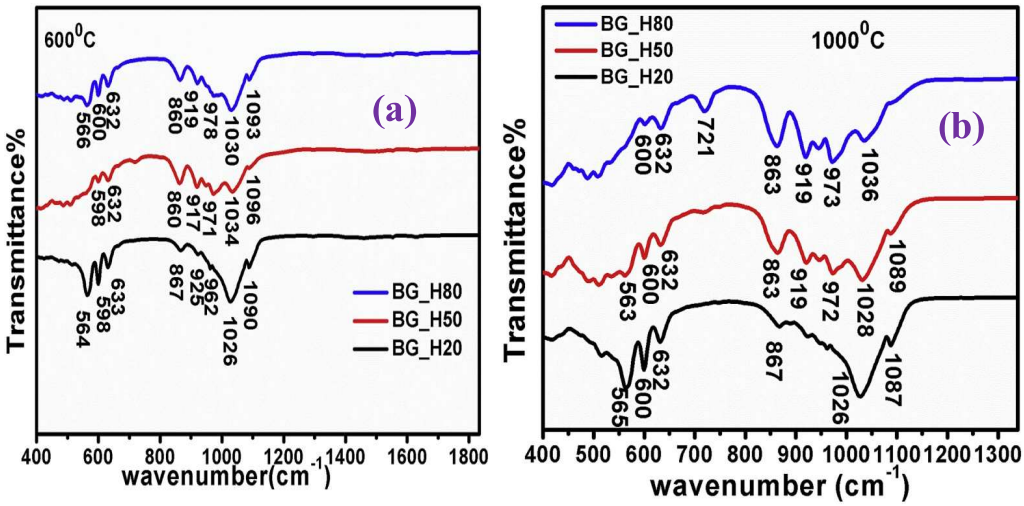


**Figure 4.5 (a)** Transmittance FTIR spectra of bioglass/hydroxyapatite composite heated at 600°C and **(b)** at 1000°C.

## 4.6 In-vitro bioactivity analysis

Immersion of samples in the SBF solution leads to hydroxyapatite layer formation over the surface which is characterized by XRD, FTIR, and SEM. **Figure 4.6 (a),** and **Figure 4.6 (b)** shows the FTIR results of sintered bioglass/hydroxyapatite composite after immersion in SBF. In **Figure 4.6 (a)**, for BG_H20 composite, sintered at temperature 600°C, the intensity of phosphate bands present at 561,600, 1033 and 1090 $cm^{-1}$ started to decrease in SBF (after 14 and 21days) which shows the degradation in the composite. Besides this, carbonate ions at 866 $cm^{-1}$ and O-H ion at 634 $cm^{-1}$ also showed decreased intensity after immersion proving the degradation of the composite. Up to 21 days immersion, some bands disappeared in the spectrum which indicates the results after the dissolution of ions in SBF. After 28 days, bands of phosphate, carbonate, and O-H were again formed which indicates the formation of hydroxyl carbonate apatite layer (HCA). For BG_H50 composite sintered at temperature 600°C, the phosphate bands ($PO_4^{-3}$) at 561,600 1033 and 1090 $cm^{-1}$ were sharp after 14 and 21 days immersion than before immersion in SBF which indicates the formation of apatite layer of calcium phosphate. The carbonate band at 870 and 1420 $cm^{-1}$ decreased after SBF immersion which indicates the dissolution of some ions like Mg ions in bioglass structure (Lopes et al., 1998**,** Lu et al., 2019) and formation of hydroxyl carbonate apatite layer (HCA) over the surface. During immersion in SBF, changes in band intensity confirm the formation and dissolution of apatite. Magnesium present in bioactive glass acts as a substitution in the apatite layer which increases the dissolution rate in SBF (Brückner et al., 2016). For BG_H80 composite, the intensity of phosphate, carbonate, and hydroxyl ions is high after immersion as compared to before immersion and peaks get more intense with increase in the immersion time in SBF up to 21 days which confirms the formation of hydroxyl carbonate apatite (HCA) over the surface. After increasing immersion time (28days), bands again start to decrease as compared to after 21 days which indicates the

dissolution of some ions in SBF. The deposition of phosphate ions over the composite surface proves the bone-like apatite layer formation over composite surfaces.

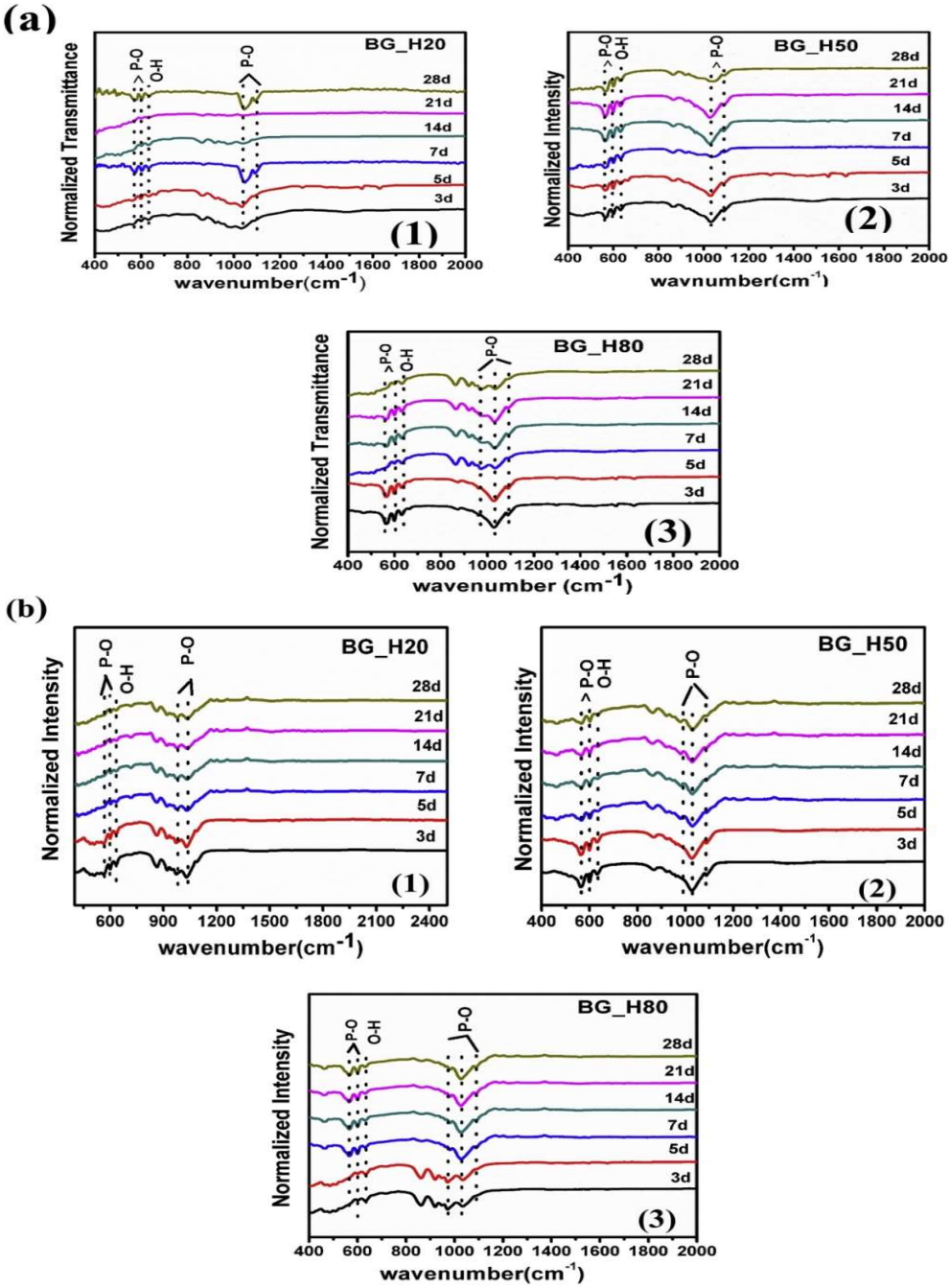


**Figure 4.6 (a)** FTIR results of sintered bioglass/hydroxyapatite composite at 600°C and **(b)** at 1000°C after immersion in SBF (1,2,3 for BG_H20, BG_H50 and BG_H80 respectively).

**Figure 4.6 (b)** depicts the FTIR behavior of immersed composite samples sintered at 1000°C for different time intervals. All composite samples showed apatite formation also confirmed in XRD but no major change in transmittance spectra was observed after immersion in SBF which shows that apatite layer deposition became stable. Comparing with before and after immersion, it was found that the intensity of peak at 1028 $cm^{-1}$ of asymmetric stretching vibration mode of $PO4^{-3}$ group decreased after immersion.

**Figure 4.7 (a)** and **Figure 4.7 (b)** depict the XRD pattern of sintered composite samples in SBF solution after immersion. All sintered composites showed hydroxyapatite phase formation after immersion. Hydroxyapatite phase was present in the composite before immersion meanwhile peaks became sharper after immersion which confirms apatite formation ability of composite. In **Figure 4.7 (a)**, after immersion, all peaks are corresponding to the hydroxyapatite phase which confirms the apatite formation after immersion.

In **Figure 4.7 (b)**, BG_H20 composite, sintered at 1000°C, the hydroxyapatite peak intensity at 31.7° increased after 5 day immersion as compared to before immersion which confirms the apatite formation. But increasing immersion time, decreased hydroxyapatite peak intensity was observed. For BG_H50 and BG_H80 composite, hydroxyapatite peak became intense after immersion as compared to before immersion which confirms the apatite formation just after immersion. Several studies suggested that crystallization reduces the bioactivity of bioglass. To improve bioactivity, hydroxyapatite was added in this study and results indicate the improved apatite ability after immersion.

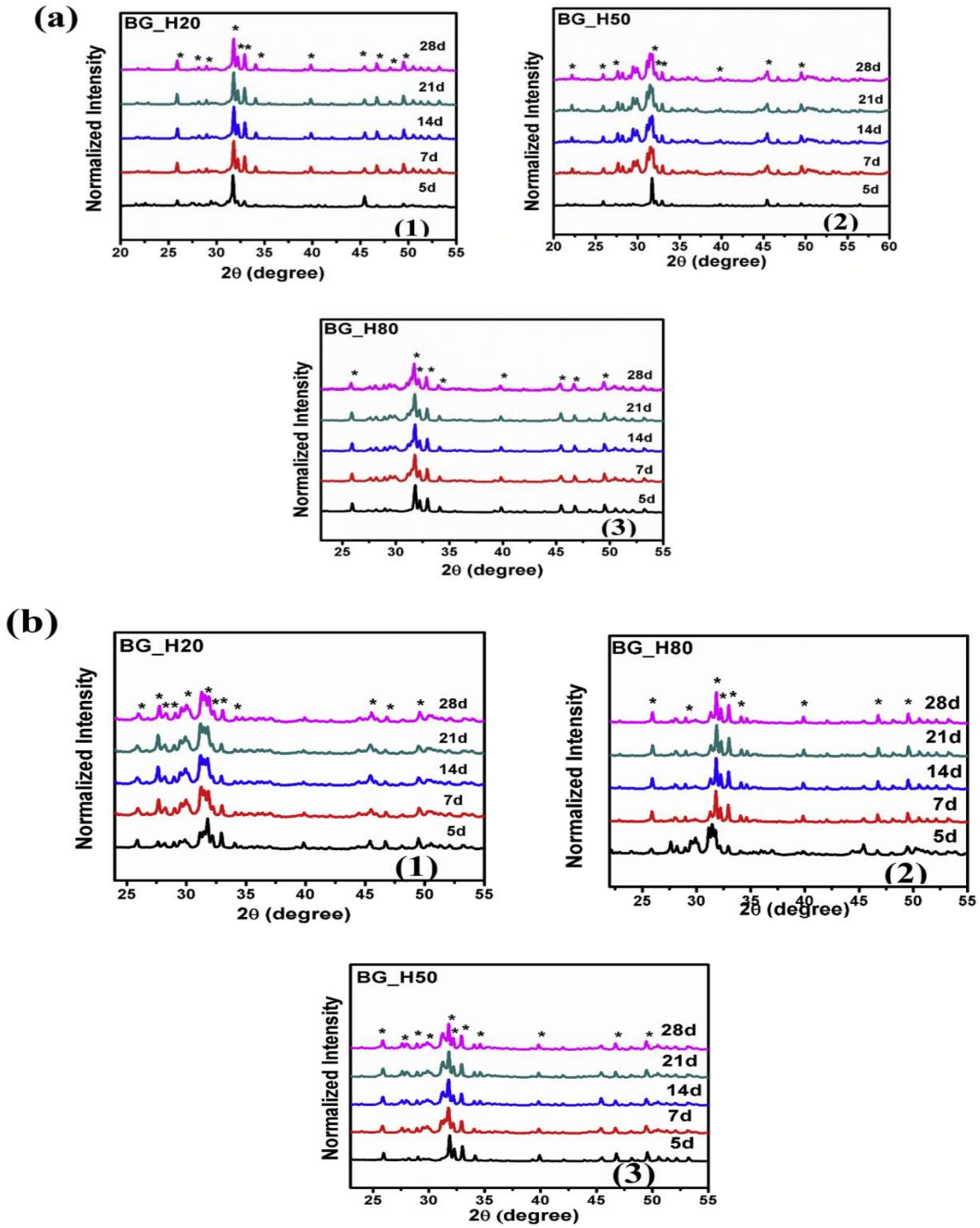


**Figure 4.7 (a)** XRD of sintered composites at 600°C and **(b)** at 1000°C in SBF solution after immersion (1, 2, 3 for BG_H20, BG_H50 and BG_H80 respectively. * shows Hydroxyapatite peak).

**Figure 4.8** shows the SEM images of composites sintered at 1000°C after 7 and 28 days immersion in SBF. As seen in the SEM image, the apatite layer was deposited on the surface which leads to pore filling (Manafi et al., 2019).

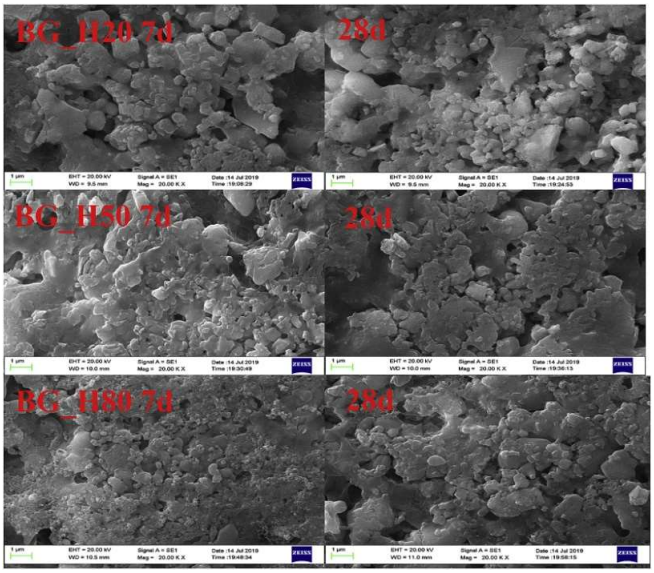


**Figure 4.8** SEM of composites sintered at 1000°C after 7 and 28 days immersion.

### 4.6.1 pH analysis

**Figure 4.9 (a)** and **Figure 4.9 (b)** shows the pH change for sintered biocomposite samples during immersion in the SBF up to 28 days. The initial pH of SBF was kept 7.40 for all samples. For all composite samples, pH has an increasing tendency up to 5days which attributed to the exchange of ions such as $Na^{+}$, $Ca^{+}$, $K^{+}$, etc present in the samples with cations of SBF ($H^{+}$ or $H_3O^{+}$) and form a negatively charged surface which attracts $Ca^{+2}$ ions present in SBF. The phosphorus and calcium present in the sample start the formation of the apatite layer over the surface and decrease the pH (Fathi et al., 2007) (Li et al., 2005). On further increasing the immersion time, the pH of SBF remains almost constant. The deposition of the hydroxyapatite layer was confirmed in XRD and FTIR analysis.

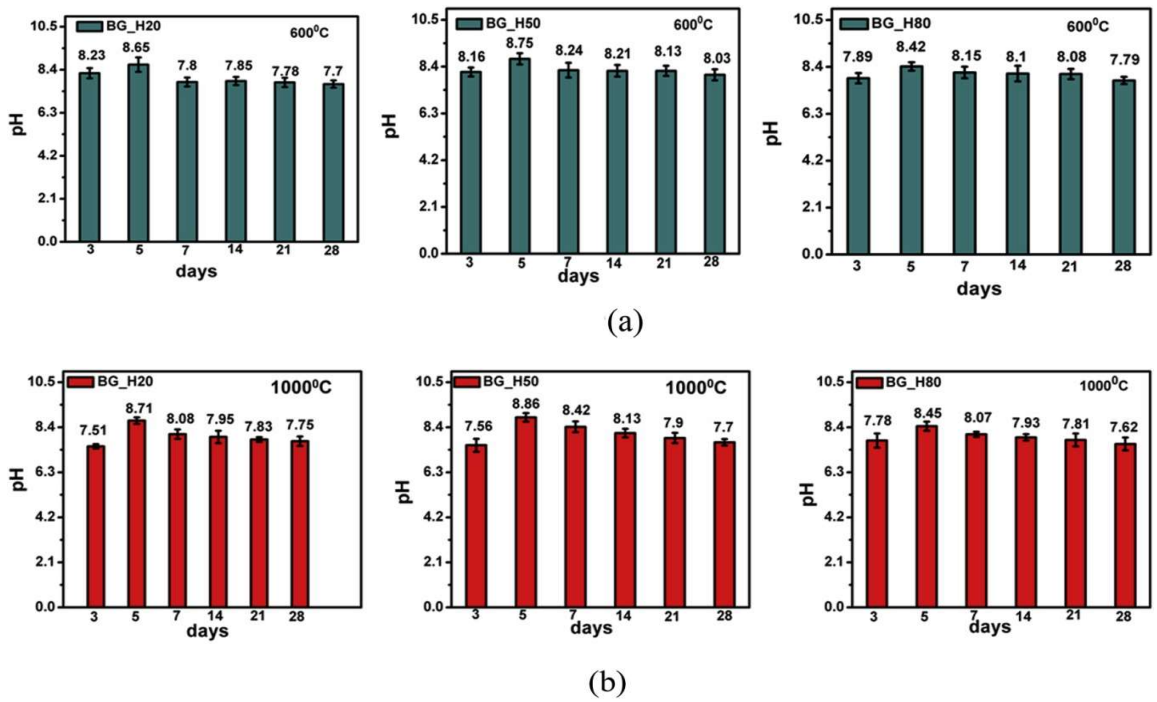


**Figure 4.9 (a)** pH changes for sintered composites at 600°C and **(b)** at 1000°C during immersion.

Physical (density) and mechanical properties

## 4.7 Physical (density) and mechanical properties

**Table 4.3** shows the relation between the density and compressive strength of bioglass/hydroxyapatite composite sintered at 600 and 1000°C. In terms of density, results show that the incorporation of hydroxyapatite in bioglass leads to increase in density with increase in sintering temperature. This increasing trend was due to the higher density of hydroxyapatite than bioglass. Sample BG_H80 shows maximum bulk density at both

sintering temperatures because of the hydroxyapatite amount. An increase in sintering temperature also increases the density of composite. As hydroxyapatite content increases, the porosity also decreases due to increase in density. Composite samples sintered at 600°C shows a lower density than samples sintered at 1000°C. At 600°C, the density of composite samples was found 2.52, 2.75 and 2.88 g/cc for BG_H20, BG_H50 and BG_H80 samples respectively. Also enhanced densities of composite samples were found at 1000°C which were 2.74, 2.90 and 2.98 g/cc for BG_H20, BG_H50 and BG_H80 samples respectively. Lopes et al., 1999 reported that increment in the density of composite can be explained by the fact that with increase in temperature the viscosity of glass reduces which increases the mass transport mechanism between the hydroxyapatite and glassy phase.

The mechanical properties of composite materials depend upon the porosity and sintering temperature. With an increase in sintering temperature, composites show an increase in compressive strength with decrease in porosity. Composites sintered at 600°C and 1000°C show an increase in compressive strength range from 34 MPa to 52 MPa. An increase in compressive strength improves the load-bearing capacity and makes the implant for resisting the trauma.

**Table 4.3** Density and compressive strength of the sintered composite sample.

| Sample code | Bulk density (600°C)g/cc | Compressive strength (MPa) | Bulk density (1000°C)g/cc | Compressive strength (MPa) |
|---|---|---|---|---|
| BG_H0 | 2.50 | 34.44 | 2.66 | 38.45 |
| BG_H20 | 2.52156 | 37.512 | 2.7455 | 42.29 |
| BG_H50 | 2.75285 | 41.156 | 2.9064 | 47.26 |
| BG_H80 | 2.88431 | 44.012 | 2.9822 | 52.13 |

## 4.8 Biocompatibility analysis

**Figure 4.10** shows the biocompatibility of sintered composites in terms of % cell proliferation with cell line MG-63 for 2 and 7 days using MTT assay. An increase in cell proliferation was observed in both sintered samples and found increased for samples sintered at 1000°C as compared to 600°C except BG_80 for day7 which shows that an increase in sintering temperature promotes cell proliferation on composite. The proliferation activity for BG_20, BG_50, BG_80 (sintered at 600°C) and BG_20 (sintered at 1000°C) was found significantly lower as compared to control for day 2. However, sample BG_80 (sintered at 1000°C) shows significantly higher proliferation value as compared to control for a similar time of incubation. Results also indicate that % Cell proliferation value for all sintered composite samples increases with an increase in culture days and no toxic effect was found on MG63 cell proliferation. Although it was found that composite BG_H50 (sintered at temperature 1000°C) has maximum cell viability of about 121% and BG_H80 (sintered at 600°C) with 122% after 7 days incubation in the culture medium as compared to control. After 7 days of incubation, the sample BG_20 (sintered at 600°C) shows significantly lower value as compared to control. However, BG_80 (sintered at 600°C) and BG_50 (sintered at 1000°C) show significantly higher proliferation than control. In composites sintered at 600°C; the BG_80 and, in composites sintered at 1000°C, the BG_50 exhibit the highest proliferation of MG-63 cells. These findings indicate that the substituted bioactive glass with the hydroxyapatite composite system promotes cell growth.

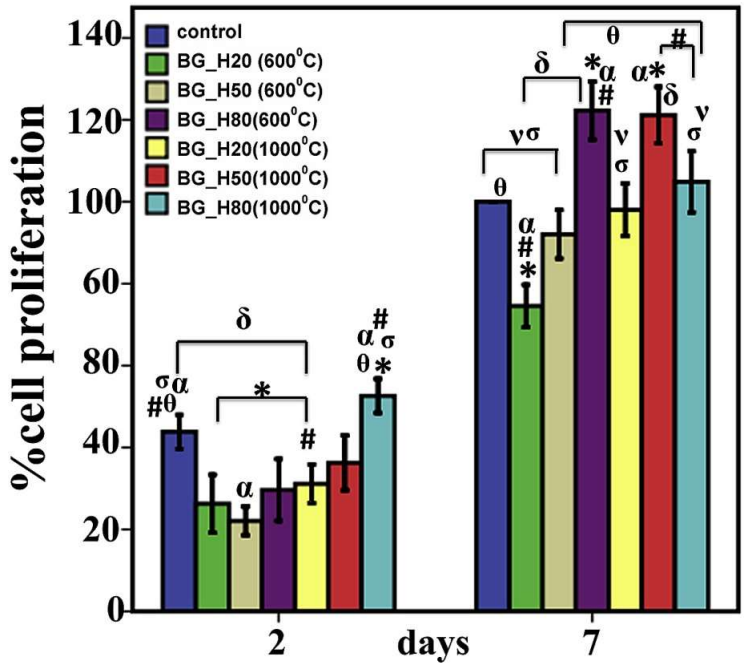


**Figure 4.10** Biocompatibility of sintered composites in terms of % cell proliferation with cell line MG-63.

## 4.9 Conclusion

The present investigation was carried out to understand the behavior of sintering temperature on zirconia substituted bioactive glass and hydroxyapatite biocomposite system in terms of structure, bioactivity, cell proliferation, and physical properties. The substituted bioactive glass of amorphous nature was mixed with prepared hydroxyapatite and sintered. The amorphous nature of bioactive glass tends to crystallize because of sintering. All composites show improved bioactivity. Sintering promotes cell proliferation in the composite system and found better in composites sintered at 1000°C than sintered at 600°C. Several researchers reported that crystallization in bioglass reduces the apatite layer formation ability. To improve this property, hydroxyapatite was added in the bioglass system and results show improved bioactivity.